Available online at www.sciencedirect.com
SCIENCE DIRECT®
Journal of Sound and Vibration 268 (2003) 1025–1035
JOURNAL OF SOUND AND VIBRATION
www.elsevier.com/locate/jsvi

Letter to the Editor

Analysis of the aeroacoustic characteristics of the centrifugal fan in a vacuum cleaner

Wan-Ho Jeon*, Seung-Jo Baek, Chang-Joon Kim

Core Technology Group, Digital Appliance Research Lab., LG Electronics Inc., 373-23 Kasan-dong, Keumchon-gu, Seoul 153-802, South Korea

Received 17 June 2002; accepted 17 March 2003

1. Introduction

The centrifugal fan, widely used in home appliance electrical machines causes a serious noise problem. Especially, the centrifugal fan used in a vacuum cleaner produces a high-level noise due to its high rotating speed. The centrifugal fan has an impeller, a diffuser and a circular casing. As the size of an impeller becomes smaller, its rotating speed needs to be increased to meet required performance specification, and therefore, the aerodynamic force applied on the impeller blades becomes severer. This unsteady aerodynamic force may generate excessive noise to the environments. Among the various noise sources in the centrifugal fan of a vacuum cleaner, the flow interaction between the rotating impeller and stationary diffuser vane plays a major role in generating the strong tonal noise. In addition, the flow separated at the impeller blades and the inflow turbulence contribute to the broadband noise. Due to the small gap between the impeller and diffuser, the sound pressure levels at blade passing frequency (BPF) and its higher harmonic frequencies are dominant in the noise spectrum of the vacuum cleaner.

As the control and the reduction of the noise from vacuum cleaners are essential requirements for the fan design, various noise reduction methods have been studied for the last three decades [1–4]. Earlier works mostly focused on identifying the dominant noise generation mechanism for the centrifugal fan and suppressing the generated noise [1,2]. Neise summarized the efforts in reducing the blade passage tone by changing the geometry of the impeller and the cut-off [1,2]. Sugimura and Watanabe discussed the resonance phenomena at the impeller passage and the noise reduction method for the centrifugal fan [3]. Lauchle and Brungart changed the regular pitched impeller blade to the uneven pitched impeller configuration in order to reduce the tonal noise [4]. However, these methods should be carried out in the final stage, i.e., after the design and the manufacturing process of the impeller are finished. The noise reduction process may be very time and money consuming work. Thus, we need to develop a method to predict the sound

*Corresponding author. Tel.: +82-2-818-7993; fax: +82-2-867-9629.
E-mail address: whjeon@lge.com (W.-H. Jeon).

0022-460X/03/$ - see front matter
doi:10.1016/S0022-460X(03)00319-5

pressure field numerically so that it can be implemented approximately during the design stage of the centrifugal fan.

A fan designer needs a fast and reasonably accurate solver for the flow and sound field analysis. In the design stage, the aeroacoustics of the designed fan is analyzed, and if the predicted sound pressure level exceeds the design limit, some relevant design parameters of the impeller should be changed to meet design requirements. In order to predict the sound pressure field for the centrifugal fan, the detailed information on the unsteady flow needs to be calculated. But, conventional computational fluid dynamics (CFD) requires a large amount of meshes and significant CPU times to analyze the unsteady flow field. Most traditional CFD techniques need several weeks to obtain reliable unsteady flow-field data. This time-consuming aspect makes it impractical to adopt this approach especially in the design stage. To overcome this problem, we use a two-dimensional vortex method to analyze the unsteady flow field of the centrifugal fan. Vortex method has been widely used in calculating the unsteady flow field of the turbomachines [5,6]. The impeller and diffuser vanes are modelled as point vortices and the surrounding casing is modelled as source panels. The sound pressure level of the centrifugal fan can be predicted by using the calculated unsteady force data in the fan flow region. The aeroacoustic pressure is calculated by Ffowcs–Williams and Hawkings (FWH) equation. In that equation, only dipole term is considered because the other terms like monopole and quadrupole may not largely affect on the sound generation compared to the dipole term [7,8]. The acoustics generated by the moving impeller blades and flow interactions in the stationary diffuser are calculated separately.

2. Numerical methods

2.1. Centrifugal fan used in a vacuum cleaner

The centrifugal fan considered in this study has an impeller and a diffuser, which have nine blades and 16 vanes, respectively. The outlet diameter of the impeller and the inlet diameter of the diffuser are 0.109 and 0.112 m, respectively. The outlet blade angle with respect to the circumferential direction is 25.0°, and the position of the maximum camber is 45% chord length from the leading edge of the blade. The inlet and outlet angles of the diffuser vane are 4.0° and 14.5°, respectively. A solid modelling view of the designed impeller and diffuser is shown in Fig. 1. Fig. 2 shows the centrifugal fan assembled with an universal AC motor. The motor is located at the lower part of fan, and the impeller is connected to the motor part by a shaft.

The sound generated from the vacuum cleaner is mostly aeroacoustic which is related to the flow rate and the high rotating speed of the impeller. The small clearance between the impeller tip and the inlet diffuser vane, which is an important design parameter for the performance, makes the tonal sound dominant in the centrifugal fan.

The measured acoustic pressure spectrum from the centrifugal fan, which was being operated at 26 760 rpm, is shown in Fig. 3. One microphone was located 1 m apart from the center of the centrifugal fan unit in the x direction. Another microphone was located 1 m apart in the y direction. The two measured sound pressure spectra are similar due to the symmetric geometry of the impeller and diffuser. However, some differences are shown due to the asymmetric flow path and the motor casing, therefore the radiated sound pressure reveals to have some directivity

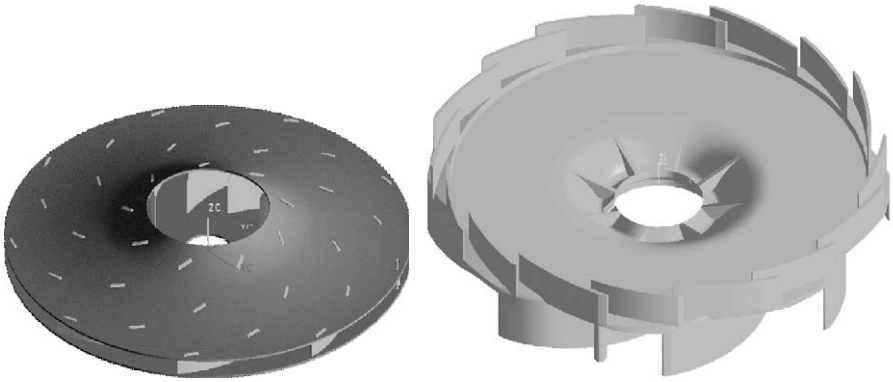

Fig. 1. Schematic view of the impeller and the diffuser.

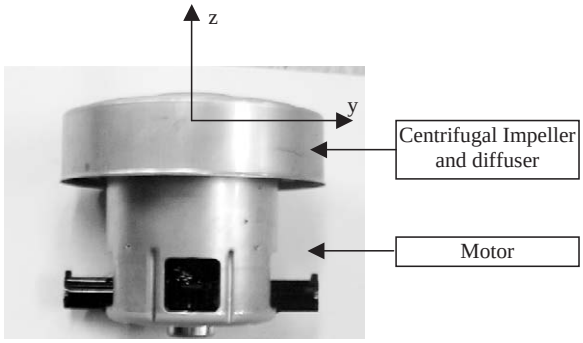

Fig. 2. The centrifugal fan unit of a vacuum cleaner.

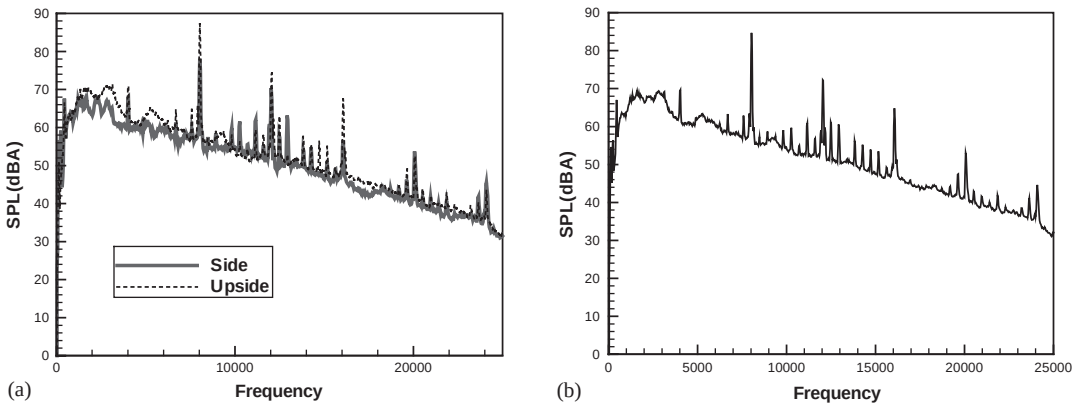

Fig. 3. Measured acoustic spectrum which is measured at 1 m apart. (a) Spectrum measured from the side and upside directions. (b) Averaged SPL of the measured spectrum from both sides.

pattern. The averaged spectrum of the two in Fig. 3(b) is used to compare to the numerical results. The peaks at BPF (4014 Hz) and its harmonics (8028, 12042 Hz) are noticeable clearly. The sound pressure level of the tonal noise at BPF is 25 dBA higher than that of the broadband noise.

2.2. Analysis of the flow in the centrifugal fan

The centrifugal fan is modelled as three major components; the impeller, the diffuser and the circular casing as show in Fig. 4. In Fig. 4, Q means the inlet flow rate, *Si* means the impeller blade, *Dif* means the diffuser blade and *Cas* indicates the casing. The impeller transfers mechanical energy to the flow, and the diffuser recovers the static pressure from the accelerated impeller exit flow through diffusing process, and the casing collects and redirects the flow into the motor core part for cooling. The flow is finally exhausted into the ambient air through the outlet holes on the case.

It is assumed that the impeller rotates at a constant angular speed, and the flow is incompressible and inviscid. The impeller has *NB* blades and each blade has *nc* vortex elements. Bound vortices are located at $\frac{1}{4}$ point of each element. Control points are taken at $\frac{3}{4}$ location of each element. Wake vortices are shed at the trailing edge of the impeller and the diffuser at every time step to satisfy the Kelvin's theorem. Shed vortices are convected with the local induced velocity. The inlet flow is modelled as a point source located at the center of the fan. The casing is modelled as constant source panels, for which the control points are taken at the center of the element. In order to complete the two-dimensional model, outlet is modelled as sink panels. Sink panels are circular and located at $0.97D$. The vortex particles, which cross the sink panels, are removed from the calculation domain.

The induced velocity at $\vec{x}_{cj}$ is composed of four components, as shown in Eq. (1)

$$\vec{U}(\vec{x}_c;t) = \vec{U}_Q(\vec{x}_c;t) + \vec{U}_{bv}(\vec{x}_c;t) + \vec{U}_{wv}(\vec{x}_c;\vec{t}) + \vec{U}_{sp}(\vec{x}_c;t). \tag{1}$$

The four terms represents the velocity at $\vec{x}_{cj}$ induced by the point source, Q, the bound vortices of the impeller and diffuser, the wake vortices, and the source panel, respectively.

Unknown strengths of the bound and wake vortices and source panels are calculated with the normal boundary condition, i.e., there is no flow across the surface boundary (Eq. (2)) and

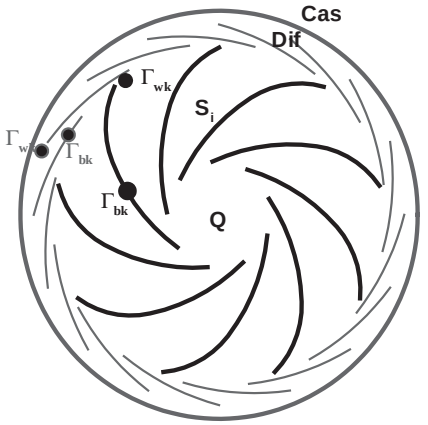

Fig. 4. Configuration of the centrifugal fan with the circular casing.

Kelvin's theorem (Eq. (4)) [6]

$$g(\vec{x}_c;t)_j \equiv \vec{U}(\vec{x}_c;t)_j \cdot \vec{n}(\vec{x}_c)_j = \begin{cases} \Omega(\vec{n}(\vec{x}_c)_j \times \vec{x}_{cj}(t)), & \vec{x}_{cj}(t) \in S_i(t), \\ 0, & \vec{x}_{cj}(t) \in Dif \ \ \& \ \ Cas, \end{cases} \quad i = 1, K, Z. \tag{2}$$

Combining Eq. (1) with Eq. (2) results in

$$\left[\vec{U}_Q(\vec{x}_c;t)_j + \vec{U}_{bv}(\vec{x}_c;t)_j + \vec{U}_{wv}(\vec{x}_c;t)_j + \vec{U}_{sp}(\vec{x}_c;t)_j\right] \cdot \vec{n}(\vec{x}_c)_j - g(\vec{x}_c;t)_j = 0, \tag{3}$$

$$\frac{D\Gamma_m(t)}{Dt} = 0, \qquad \left[\sum_{k=1}^{nc} \Gamma_{bk}(t) + \sum_{k=\ 1}^{nv} \Gamma_{wk}(t)\right]_m = 0, \tag{4}$$

where Γ_m is the total circulation of mth blade, which includes the circulations of bound vortices of the blade (Γ_b) and wake vortices (Γ_w), where m, nc and nv means the numbers of blades, elements at each blade, and shed vortex particles, respectively.

The convection of the vortices shed at the trailing edge is calculated by second order Runge–Kutta method.

The force on each element of the blade is calculated by the following unsteady Bernoulli equation:

$$\vec{F}_{nj} = \rho\left\{\vec{U}(\vec{x}_c) \cdot \vec{\tau}_j \frac{\Gamma_{bj}}{\Delta s_j} + \frac{\partial}{\partial t} \sum_{k=1}^{j} \Gamma_{bk}\right\} \Delta s_j, \tag{5}$$

where, $\vec{F}$, $\vec{\tau}$ and Δs_j are the normal force on the element, the tangential vector of the element, and the length of that element, respectively. ρ is the density of working fluid.

2.3. Analysis of the noise of the centrifugal fan

Neise showed that especially the dipole which results from the unsteady force fluctuation is the dominant source of the fan noise [7]. The most prominent source of the dipole in the centrifugal fan is the rotating impeller. Therefore, the sound field generated by the forces of the impeller and diffuser blades is considered in this study.

Eq. (6) represents the inhomogeneous wave equation following FWH, which can be derived from the basic fluid dynamic equations using generalized functions

$$\left(\frac{1}{a_0^2}\frac{\partial^2}{\partial t^2} - \frac{\partial^2}{\partial x_i^2}\right) p' = \frac{\partial}{\partial t}[\rho v_n \delta(f) \nabla f] - \frac{\partial}{\partial x_i}[n_i p \delta(f) \nabla f] + \frac{\partial^2}{\partial x_i \partial x_j}[T_{ij} \mathrm{H}(f)], \tag{6}$$

where, p' is the sound pressure (Pa), ρ the air density (kg/m^3), n_i the surface normal, a_0 speed of sound (m/s), v_n the normal surface velocity (m/s), p the static pressure (Pa), T_{ij} the $\rho u_i u_j + P_{ij} - a_0^2 \rho \delta_{ij}$ the Lighthill tensor (Pa), $\delta(f)$ the Dirac-delta distribution and $\mathrm{H}(f)$ is the Heaviside distribution.

The first, second and third terms in the right-hand side of Eq. (6) represent monopole, dipole and quadrupole, respectively. Only dipole term in Eq. (6) is considered in this study, and the force is modelled as the point force as described earlier. Then Eq. (6) can be simplified to Eq. (7)

as follows:

$$P' = \left[\frac{x_i - y_i}{4\pi a_0 r^2 (1 - M_r)^2}\left\{\frac{\partial F_i}{\partial t} + \frac{F_i}{1 - M_r}\frac{\partial M_r}{\partial t}\right\}\right], \tag{7}$$

where

$$M_r = \frac{M_i r_i}{r}. \tag{8}$$

F_i is calculated force of the impeller blade and a_0 is the speed of sound. x_i and y_i are the source position and absorber position and r is the distance between them. This formulation was first derived by Lowson [9] in 1965, and indicates that the acoustic pressure by the moving point force can be calculated using the time variation of the force and acceleration. By applying this equation to each blade element, we can predict the acoustic pressure in the free field. The effect of the scattering, reflection and refraction as well as the casing on the sound field is not considered in this analysis. Therefore, only the behavior of the noise source and its radiation to the free field is calculated in this study.

The target frequency range is about 5–15 kHz, and the corresponding wavelength is about 2.27–6.8 cm. Because the wavelength is comparable to the impeller radius, it is necessary to consider the transition frequency of the impeller and the blade, which is defined in Eq. (9)

$$f_{imp} = a_0/D, \quad f_{bl} = a_0/C, \tag{9}$$

where D is the outlet diameter of impeller and C is the camber of blade. If the target frequency range is smaller than the f_{imp}, the impeller can be considered as a point source. If the target frequency is smaller than the f_{bl}, each impeller blade can be considered as point forces. In this case, the target frequency is higher than f_{bl}, therefore we need to divide the each blade into many elements.

3. Numerical results

3.1. Analysis of unsteady flow field

The impeller has nine blades and rotates at about 26 766–29730 r.p.m. The impeller diameter and blade angle are 0.035 m and 17.0° at inlet. At outlet, they are 0.109 m and 25.0°. The diffuser has 16 vanes, and the inlet and outlet vane diameters are 0.112 and 0.124 m, respectively. The volume flow rate is 1.36–2.526 m^3/min. During the analysis of the unsteady flow calculation, overall fan performance is calculated as the total head between the impeller inlet and the diffuser outlet as shown in Fig. 5. Volume flow rate was 2.526 m^3/min, and the mean head was calculated as 1560 m (1874.5 mmAq). The measured suction pressure of the fan was 1147 mmAq. Because the proposed method does not take account of the viscous loss effect, the calculated head shows deviations from the measured value.

Fig. 6(a) shows the strength of shed vortex at one impeller blade as a function of the revolution of the impeller. During one revolution of the impeller, the strength of shed vortex fluctuates periodically 16 times. On the other hand, the vortex strength at the diffuser vane fluctuates

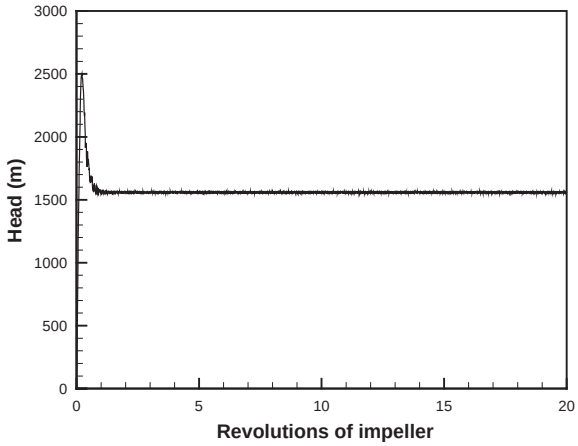

Fig. 5. Variations of calculated total head.

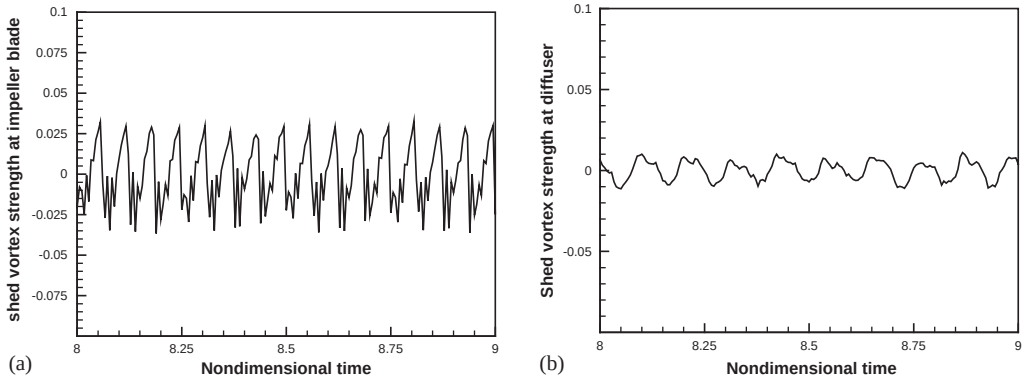

Fig. 6. Variations of shed vortex strength at each blade tip. (a) Shed vortex strength from the impeller blade. (b) Shed vortex strength from the diffuser vane.

periodically 9 times as shown in Fig. 6(b). These periodic fluctuations at the impeller and diffuser produce tonal sound.

In Fig. 7, the magnitude distribution of the calculated absolute velocity is shown at some selected time steps. The impeller rotates counter-clockwise. As the blade tip comes closer to the leading edge of diffuser vane, the negative vortices strength at the blade tip becomes higher.

The calculated force on each blade of the impeller is decomposed into the x- and y-axis components as shown in Fig. 8(a). Force components in each direction show periodic change with a period of 0.00224 s. The interaction between the forces on impeller blades and diffuser generate total force fluctuations with higher frequency as can be seen in Fig. 8(a). The total force fluctuates 16 times per one revolution in Fig. 8(a). In Fig. 8(b), the force variation on each vane of the diffuser is shown. The force on the diffuser vane fluctuates 9 times per one revolution of the impeller.

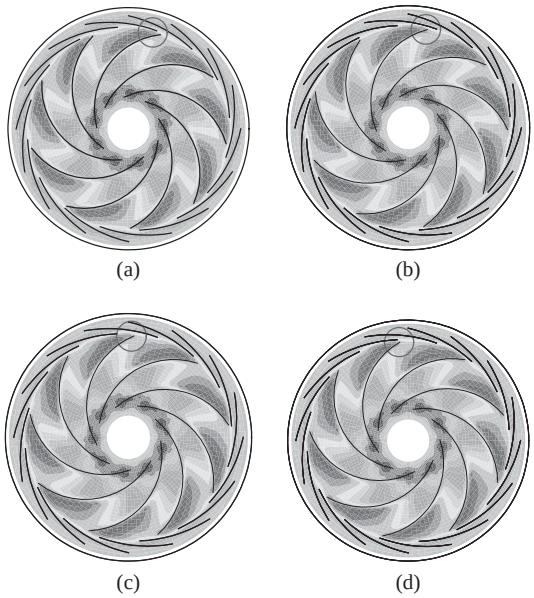

Fig. 7. Magnitude of the absolute velocity. (a) time/$T = 6.0$, (b) time/$T = 6.022$, (c) time/$T = 6.044$ and (d) time/$T = 6.066$.

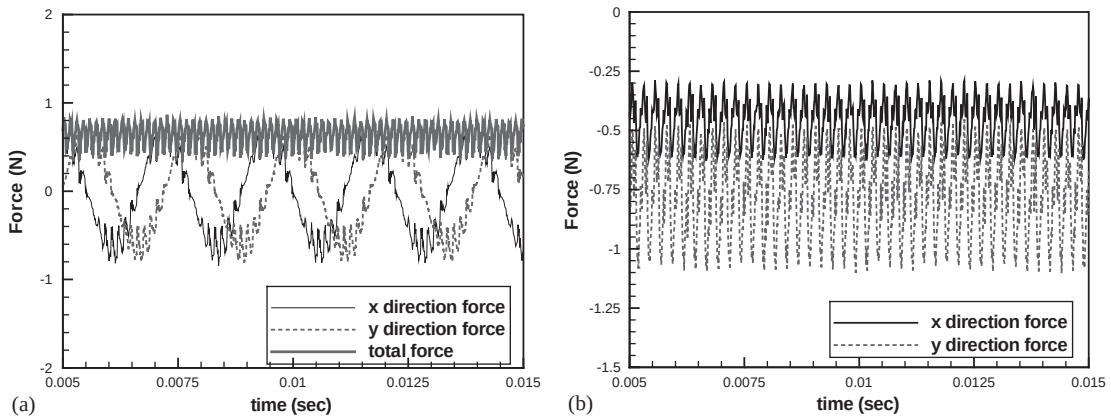

Fig. 8. Variations of the calculated force for one blade of the impeller and diffuser. (a) Force variation on one blade of impeller. (b) Force variation on one diffuser vane.

Because the force and its time derivative are the main sources of the sound pressure (see Eq. (7)), it will be interesting to see the time derivative of force variation on the impeller as shown in Fig. 9. 16 pulses per one revolution of impeller can be clearly seen in Fig. 9(a), and nine pulses of the time derivative of force on the diffuser in Fig. 9(b). By comparing the force and its time derivative, it can be judged that the time derivative of the force is the dominant source of the aeroacoustic noise.

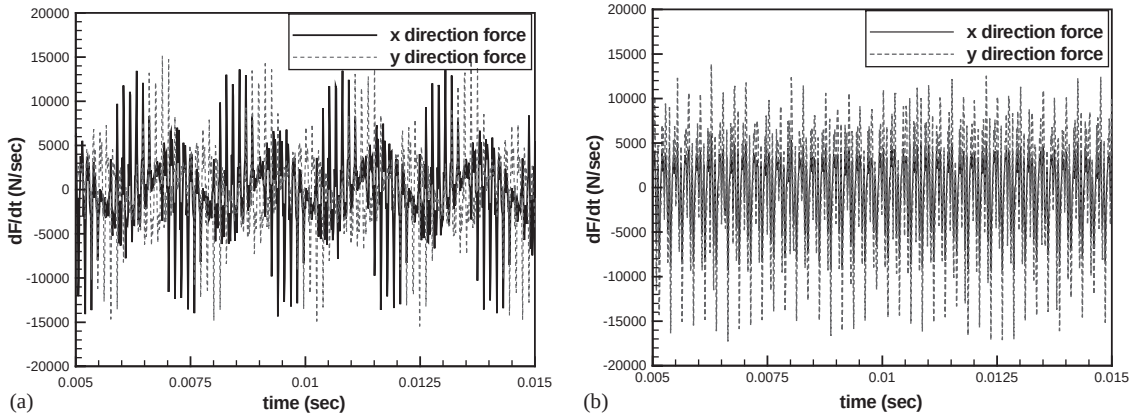

Fig. 9. Variations of the calculated time derivative of the force on one blade of the impeller and diffuser. (a) Time derivative of the force on one impeller blade. (b) Time derivative of the force on diffuser vane.

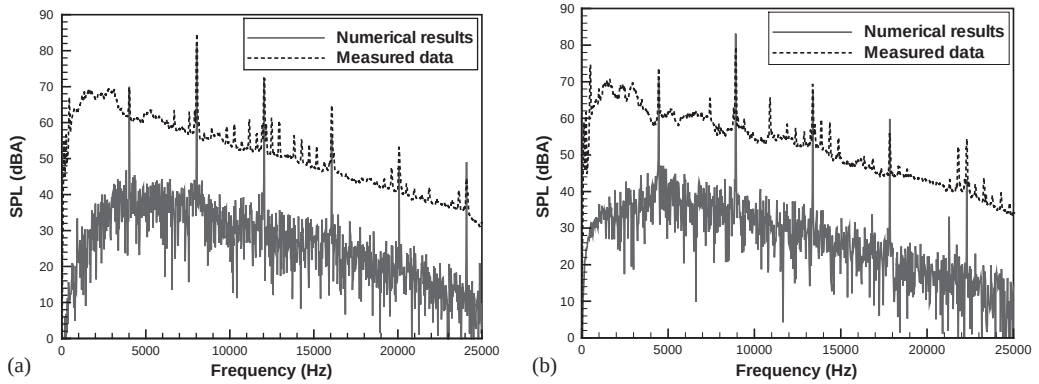

Fig. 10. Comparison of the predicted and measured sound pressure levels. (a) 26 760 r.p.m. case and (b) 29 930 r.p.m. case.

3.2. *Analysis of the aeroacoustic noise in the centrifugal fan*

In Fig. 10(a), the predicted sound pressure level at (1,0,0) location is compared with the measured one when the impeller rotates at 26760 r.p.m. In Fig. 10(a), the peak level at second BPF (8028 Hz) is much larger than that at BPF (4014 Hz). The level of broadband noise shows large differences because the prediction method does not consider the effect of the turbulent boundary layer, separated flow and the inflow turbulence, which mainly generate the broadband noise. They can be approximately calculated if more elegant numerical flow approach such as large Eddy simulation (LES) or direct numerical simulation (DNS) for the unsteady flow-field calculation is implemented. Since the sound pressure level of the broadband noise is significantly smaller than that of the tonal noise in this centrifugal fan case, overall aeroacoustic characteristics are determined from the information of the tonal sound spectra. It is noted that the predicted and measured peak levels at BPF and its higher harmonic frequencies are very close. The detailed comparison is shown in Table 1. The predicted sound pressure level at second BPF, which is the

Table 1
Comparison of the predicted and measured peak levels (26 760 r.p.m. case)

	Measured (dBA)	Calculated (dBA)
BPF (4014 Hz)	69.3	69.5
Second BPF (8028 Hz)	84.0	80.8
Third BPF (12 042 Hz)	72.2	71.9

Table 2
Comparison of the predicted and measured peak levels (29 930 r.p.m. case)

	Measured (dBA)	Calculated (dBA)
BPF (4014 Hz)	73.3	70.0
Second BPF (8028 Hz)	79.5	83.0
Third BPF (12 042 Hz)	69.0	67.2

noisiest sound, is 3.2 dBA lower than the measured data. Fig. 10(b) shows similar results for 29 930 r.p.m. case. Again, the predicted peak levels are sufficiently close to the measured one, but the broadband noise shows about 25 dBA difference. As shown in Table 2, the predicted sound pressure level at second BPF, which is the nosiest frequency, is 3.5 dBA higher than that of measured one. Thus, it can be said that this proposed method can predict the peak sound pressure levels from the centrifugal fan within 3–4 dBA.

In order to get more detailed information on the effect of the diffuser on the total noise level, sound pressure levels were calculated with and without the diffuser. The result is shown in Fig. 11. The overall SPL, which was calculated without the diffuser, is reduced by about 2 dBA. The peak level at BPF is changed from 63.4 to 69.5 dBA, and the peak level at second BPF is changed from 83 to 80.0 dBA. The peak level at third BPF is changed from 66.5 to 71.9 dBA, and the broadband noise level increases by about 10 dBA. Therefore, the sound pressure generated from the diffuser should be considered together in order to predict the aeroacoustics of the centrifugal fan more accurately.

4. Conclusions

The new method to calculate the unsteady flow fields and aeroacoustic sound pressure in the centrifugal fan of a vacuum cleaner has been developed. Due to the highly rotating speed of the impeller and the small gap between the impeller tip and the diffuser vane, the centrifugal fan produces very high-level noise at BPF and its harmonic frequencies. In order to calculate the sound pressure of the centrifugal fan, a large amount of unsteady flow-field data is necessary. This unsteady flow-field data is calculated by the vortex method. The sound pressure is then calculated by an acoustic analogy. By using the developed method, the aeroacoustic sound in the centrifugal fan of an 1800 Watt (input power) vacuum cleaner, was calculated, and the results were compared to the measured data. The predicted tonal sound pressure levels spectra of an acoustic pressure

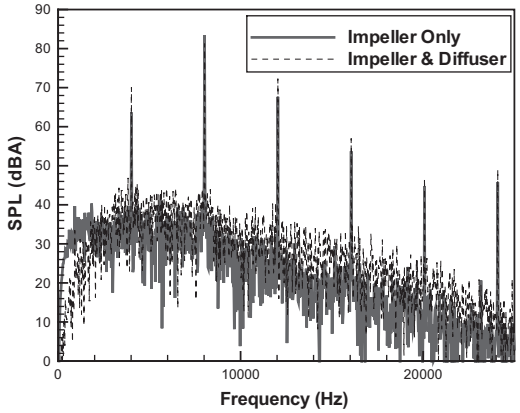

Fig. 11. Predicted acoustic spectrum with and without the diffuser.

agree very well with the measured data within 4 dBA deviation range. Due to the lack of detailed modelling on the turbulence and quadruple source the calculated broadband noise spectra show some deviation from the measured data. This can be improved by using more accurate numerical method such as LES and DNS.

References

[1] W. Neise, Noise reduction in centrifugal fans: a literature survey, Journal of Sound and Vibration 45 (1976) 375–403.
[2] W. Neise, Review of noise reduction methods for centrifugal fans, Journal of Engineering for Industry 104 (1982) 151–161.
[3] K. Sugimura, M. Watanabe, A study on suppressing acoustic resonance of interaction tones from a centrifugal motor fan, Seventh International Congress on Sound and Vibration, Germany, 2000, pp. 1259–1266.
[4] G. Lauchle, T. Brungart, Modifications of a vacuum cleaner for noise control, The 29th International Congress on Noise Control Engineering, Nice, France, 2000.
[5] R.I. Lewis, Extension of vortex method to the flow simulation of mixed-flow turbomachines, Proceedings of the Second International Conference on Vortex Method, 2001, pp. 181–187.
[6] W.-H. Jeon, D.-J. Lee, An analysis of the flow and aerodynamic acoustic sources of a centrifugal impeller, Journal of Sound and Vibration 222 (3) (1999) 505–511.
[7] W. Neise, Review of fan noise generation mechanisms and control methods, An International INCE Symposium, Senlis, France, 1992, pp. 45–56.
[8] W.-H. Jeon, S.-J. Baek, C.-J. Kim, Study on the aerodynamic noise characteristics of a centrifugal fan used in a vacuum cleaner, The Fifth JSME-KSME Fluids Engineering Conference, Nagoya, Japan, November 17–21, 2002.
[9] M.V. Lowson, The sound field for singularities in motion, Proceedings of the Royal Society of London Series A 286 (1965) 559–572.